The Geology and Geochemistry of Metavolcanic Rocks from Artoli Area, Berber Province, Northern Sudan: An Implication for Petrogenetic and Tectonic Setting

Nureldin Hassan Lissan [1], Abdallah Kodi Bakheit [2]

[1.] Faculty of Earth Resources, China University of Geosciences, No. 388 Lumo Road, Wuhan, China.
[2.] Department of Geology and Mining, College of Natural Resources, University of Juba, Khartoum, Sudan.
lissannh14@yahoo.com

Abstract: The study investigates the geology and the rock geochemistry across an area of about 1250 km2 in the vicinity of Artoli village, Berber Province, Northern Sudan, in order to determine the petrographic characteristics of the rock assemblages, their original protoliths and tectonic environment. Field and laboratory works have revealed that the study area is entirely underlain by crystalline Proterozioc basement complex, which comprises dominantly low-grade schistosed metavolcanic rocks and minor high-grade metasediments, intruded by voluminous granitiod batholiths and covered locally by Tertiary and Recent sediments. The metavolcanics are originally rocks of variable compositions mostly of basic, intermediate to intermediate-acidic volcanic rocks parentage as confirmed by the chemical classification, which classified them as differentiated rocks of andisites, basaltic-andisites with lesser amount of dacites and basalts. The discrimination diagrams constructed enabled to identify the metavolcanic rocks of the area as sub-alkaline volcanic series carrying evolutionary trends of calc-alkaline affinity in a plate tectonic setting related to island arc environment. The overall geological and geochemical characteristics of the Artoli metavolcanic rocks provided essential evidence indicating that the area is a part of the westernmost Nubian Shield, as the features are consistent with the arc accretion models postulated in Sudan, Egypt and Saudi Arabia for the Neoproterozoic evolution of the Arabian-Nubian Shield. [Journal of American Science 2010;6(8):1-13]. (ISSN: 1545-1003).

Keywords: Artoli; Tectonics N Sudan; Artoli Metavolcanics; Geochemistry ANS

1. Introduction

In NE Sudan, there are a number of Precambrian terranes of exposed metamorphic rocks (Fig. 1B); among these is the Artoli area, which constitutes the study area for this research. It lies some 56 km northeast of the River Nile coastal city of Atbara in Berber Province, N Sudan, between latitudes 18º 11´ and 18º 20´ N and longitudes 33º 55´ and 34º 05´ E, (Fig.1A) and covers an area of about 1250 km2.

The area and the adjacent terranes are not only of important academic interest in their own right, but also are related to an evolution of auriferous gold mineralization. Only few regional studies were conducted on this suite of rock series, therefore, documented systematic field, geochemical, and geochronological studies are needed in order to provide a better understanding of the mode and nature of tectonic and geological evolution of the area and its associated ore deposits. In this study, the local geochemical and petrographic details of the metavolcanic rocks integrated with their field observations are provided in an attempt to determine the geochemical affinities and tectonic significance of the area within the Arabian-Nubian Shield and Saharan Metacraton realms.

The Artoli area is located at the southern end of the Keraf-Suture (KSZ) and between the high-grade gneissic terrane of the Bayuda Desert in the west and the spurs of the Red Sea Hills in the east, thus, it is sandwiched between the reworked older crust of Sharan Metacraton and the Neoproterozoic juvenile, accreted arc terrane of the Arabian-Nubian Shield (Kröner, et al., 1987a; and Stern, 1994, Fig.1).

The Saharan Metacraton is a heterogeneous continental crust, containing abundant pre-Neoproterozoic rocks with intense Neoproterozoic remobilization, dominated by high-grade gneisses, migmatites and supracrustal rocks of ensialic geochemical affinities (Kröner, et al., 1987a; Küster and Liégeois, 2001; Abdelsalam, et al., 2002).

The eastern boundary of the Saharan Metacraton in northeastern Sudan is defined by the N–S trending, ophiolite-decorated, 500 km-long and 30-150 km wide structural belt of Keraf- Suture zone (KSZ) (Fig. 1A). This suture has been interpreted as an arc-continental, tectono-lithological suture that resulted from NW–SE oblique collision between the Saharan Metacraton and the Arabian-Nubian Shield. The (KSZ) has rock assemblage comprising; high to medium- grade gneisses, siliciclastics, carbonate-rich low-grade metasediments, ophiolitic nappes,

molasse-type sediments and post-tectonic granitoids, (Abdelsalam et al., 2002).

The Arabian-Nubian Shield (ANS) is the northern sector of the East African Orogeny formed in the Pan-African (1100-500 Ma: Kennedy, 1964; 900-450 Ma: Kröner, 1984). It comprises a vast expanse of Neoproterozoic juvenile oceanic island arc crust extending from southern Israel through western Arabia, eastern Egypt and northeastern Sudan into Eritrea and Ethiopia and bordered on the west and east by older cratonic crust. The arc terranes are believed to be intra-oceanic island arc/back arc-basin complexes (Stern et al., 1994 and Kröner et al, 1987a). The Present widely accepted idea on the geotectonic crustal evolution of the ANS is that it has been developed by lateral crustal growth dominated by subduction-related processes and ensimatic arc construction through preponderate role of repeated plate boundary convergence, formation of intra-oceanic island arc system, subsequent ocean closure, amalgamation of the arc complexes and accretion to continental crust (Stern, 1994).

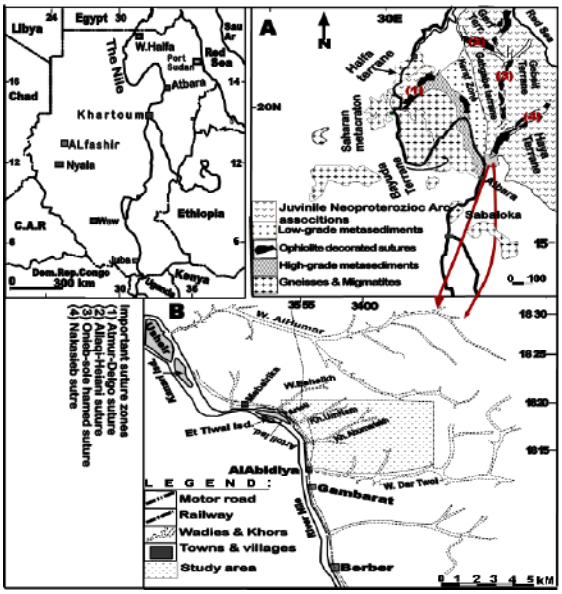

Figure 1. Locality map for; (A): A part of NE Sudan showing major terranes and important suture zones; (B): Artoli area

2. The Geology of the Study Area

The greater part of the Artoli area is underlain by crystalline basement rocks, exposed in most parts of the area except the western most (Fig. 2). The basement rocks comprise a series of spatially overlapping metamorphosed complex of schists and gneisses of volcanic and sedimentary origin cut by various generation of syn, to late-orogenic intrusive grainitiods and post-orogenic minor intrusions, all covered locally by Nubian sands and Recent superficial deposits. The contact relations among the rock types are obliterated by metamorphism and deformation, hence, integration of obvious lithological difference, metamorphic extents, field appearance and structural styles were used to classify the rock succession of the area into the following units (Fig. 2):

2.1 High-grade Metasedimentary Rocks (Paleo-Proterozoic)

Poorly defined and nearly continuous exposures of mostly high-grade metasedimentary rocks develop in the western part of the map area as a local inlier in a narrow belt extending in N-S direction (Fig. 2). The sedimentary origin of this suite, which is obvious in the field by its heterogeneous nature, frequent intercalation feature, and the short-distance facie change, is also confirmed by the geochemical and petrographic data. There is no sufficient field evidences for precise contact relations between this suite ant the other groups, as the underlying group is not exposed and the contacts with the overlying rocks are extensively modified by superimposed deformation and metamorphic events and obliterated by screes and alluvial deposits. However, the suite everywhere studied in the region ascertained to be disconformably overlying the high-grade gneisses and structurally overlain by the Low-grade volcano sedimentary series (Almond, 1982). The suite comprises variably interbedded lithologies of biotite-gneiss, quartzo-feldspathic gneiss, quartzite, marbles and amphibolites.

The biotite-gneiss, in general, is leucocratic to mesocratic, medium-grained rock exhibiting moderate gneissic layering in a NW-SE direction coinciding with the regional trend defined by parallel alignment of biotite and hornblende alternating with elongated quartz and plagioclase grains. Under the microscope the gneiss shows a simple mineral assemblage composing of angular to subangular quartz crystals within predominate orthoclase feldspars and minor plagioclase (Albite- oligoclase composition); both may be altered to turbid sericite. Of the mafic minerals, oriented yellow biotite flakes by far exceed green hornblende, muscovite and garnet. Fe-oxides are unmissed with apatite and opaques as accessories.

The quartzo-feldspathic gneiss is exposed along dry streams with the above unit at the central-west part as rather all-weathered surfaces concealed under variable thickness of alluvial sands and lag deposits. It is medium to coarse-grained, light to grayish and with detectible gneissic banding in a NW trend. Pterographically, consists of quartz, feldspars, yellowish brown biotite, few flakes of muscovite and prisms of hornblende. Secondary minerals of epidote,

sericite and chlorite are commonly developed after mafic minerals. Accessories of apatite, zircon, sphene and iron oxides are also conspicuous.

Quartzitic rocks are encountered in the eastern and the central parts of the map area as relatively outstanding ridges extending in a NE direction for considerable distance probably tracing a linear regional pattern representing fault zone (Fig. 2). The quartzites are compact, brecciated rocks or may be banded (Umtrambeish area), varying from white to ferruginous reddish brown or grey varieties. In thin section, they show abundant stout granular quartz crystals besides, few silvery muscovite flakes, plagioclase and K-feldspars.

Marbles occur in most parts of the area especially in the eastern part as irregular bands or thin layers of lenticular and tabular-shaped bodies, seldom exceed a few meters wide (0.5- 8m). Most marbles are medium to coarse-grained, massive rocks ranging from pure sugary white to impure shaded, dark gray, yellowish brown or buff coloured. However, the pure varieties show granoblastic texture, the sheared ones may show distinct cataclastic textures. 70-80 % of the rock composition is interlocking crystalline calcite with clear twin lamellae and the remaining is mostly equigranular, fine-grain quartz, sericite and plagioclase. Some mica and epidote are accessories.

Sporadic lens-shaped and patches of amphibole-rich rocks are observed in the NW part intercalating with the plutonic suite in a rather crosscutting relation and conformable with the adjacent metasediments. They are generally recognized by their dark to dark gray colour and medium-grained texture, and commonly show megascopic preferred mineral segregation banding in accord with regional trend emphasized by preferred orientation of hornblende prisms and aligned felsic minerals. The amphibolites disclose granoblastic texture and a mineral association comprising; hornblende, plagioclase and quartz as essentials, chlorite, epidote, sericite and biotite as secondary and sphene, apatite, zircon, iron oxides, garnet and pyrite as accessories ones.

2.2 The Ophiolitic Rocks (Neoproterozoic)

The occurrence of numerous dismembered fragments of obducted oceanic crust along generally NE-SW or NNE-SSW trending major belts representing suture boundaries of once existed island–arc system in the Arabian-Nubian Shield (Fig. 1A) became a general agreement among geologist nowadays (Fitches, et al, 1983; Hussein et al., 1984; Abdel Rahman, 1993). Although, Abdel Rahman, 1993, confirmed the occurrence of this suite in the study area but the present account is based merely on few insufficient filed observations, as the suite mostly lies outside the mapped area.

The term ophiolitic suite used here refers to an integrated assemblage of altered rocks found a long pinching and swelling belt (thrust bounded sheared zone) within the low-grade sequence. They represented by carbonated and serpentinized ultramafic tectonic sequence (pyroxinite and peridoditre) and retrogressed cumulous metabasic rocks mainly gabbros and banded amphibolites accompanied by altered sheeted doleritic dykes, lavas and deep sea-water sediments (Phyllitic rocks, chert and iron-rich quartzite) which may represent scattered ophiolitic fragments.

The mentioned lithologies are neither found in one stratigraphic unit nor as pure compositional varieties. The mafic-ultramafic rocks are found at scattered localities southeast and east Umtrambiesh area as strongly altered rocks of talc, talc-chlorite and chlorite-actinolite schists and serpentinites. Sheeted dykes and lavas are of great scarcity, as only scattered minute lensiod pods of lava and very small and highly altered sheets of doleritic composition found just southeast the bend of Wadi Dar Tawai (fig. 2).

2.3 Low-Grade Schistosed Metavolcanics Rocks (Neoproterozoic)

In the study area, a wide distribution of low-grade, green schist facies rocks that are predominant metavolcanics associated with relatively minor sedimentary units encountered exposed in the neighborhood of Umtrambeish ore field, in addition to small sporadic outcrops in the granitoids plain to the north (fig. 2). This group of rocks usually has a gradational boundary with the underlying units and includes metamorphosed basic to intermediate-acidic volcanic rocks that show varying degrees of deformation, ranging from massive, undeformed bodies to strongly schistosed rocks. Most of them are fine-grained with primary volcanic textures (porphyritic and sometimes amygdaloid) still recognizable. Under the microscope, most rocks contain quartz, sericitized plagioclase, chlorite and actinolite, besides K-feldspar, opaques, calcite and some rare relict pyroxene. This mineral assemblage and the shown textures are indicative features of green-schist facies metamorphism of originally volcanic rocks. Based on field and petrographic data, theses schistosed rocks are classified into; quartz-mica schist, sericite-chlorite schist and actinolite-schist.

The quartz-mica schists characterized by clear microfolds, crenulation cleavages, nearly vertical dips and well defined schistosity. They are gray to light-greenish gray coloured rocks of fine

texture and often disclose a typical low-grade mineral assemblage comprising; quartz, chlorite, muscovite, minor biotite, and subordinate sericite, plagioclase, epidote and calcite with common accessories of sphene, apatite, iron-oxides and garnet.

The sericite-chlorite schist is greenish to greenish-gray coloured rock of fine-grain texture and exhibits profound schistosity. Minerogically, it shows lepidoblastic to garnoblastic appearance in sericite, chlorite, plagioclase, quartz and minor biotite, besides epidote, iron oxides and calcite with accessory minerals of apatite, and pyrite.

The actinolite-schists are fine-gained green-coloured rocks found predominantly around Umtrambeish ore area. Under the microscope, they show almost a complete alteration testified by the high abundance of green minerals. The mineral assemblage is a combination of irregularly oriented bright green actinolite, elongated and highly altered plagioclase, dragged crystals of quartz, aggregated epidote, turbid and anhederal crystals of calcite, small, spindle-shaped granules of sphene and rounded apatite.

2.4 Syn, to Late-Orogenic Grainitiod Rocks (Neoproterozoic)

Vast masses of intermediate to acidic granitoids constitute a characteristic and dominant element of the basement rocks of the area, especially in the N and NE sectors, where they form about 50 % of the outcrops. This granitoid suite is believed to be a product of larger plutons of syn, to late-orogenic igneous activities in the late Proterozioc time that have been emplaced in both the high and low-grade sequences as evident from their xenolithic contents. Based on field and petrographic evidences, they are generally range in composition from quartz diorite, granites to micro-granites, but predominantly are hornblende granodiorites (Fig. 2).

Quartz dioritic rocks occur as excellent exposures of low to moderate relief in the NW part of the mapped area. Macroscopically, they are gray coloured rocks usually devoid of pervasive foliation, but the intense deformation caused some verities to develop a slight banding. Petrographically, they are coarse hypidiomorphic rocks in which felsic minerals constituent more than 60 %, of which quartz form about 10 %, the other minerals are slightly sericitized plagioclase, coarse subhedral hornblende, as main primaries, oriented pale-brown pleochoric biotite, mostly untwined orthoclase and perthites as minor phase and sphene, zircon, apatite, pyrite and magnetite as accessories. Secondary minerals are sericite, chlorite, epidote and carbonates.

Granodiorites constitute a wide range of rocks found in association with minor granites in the central part of area (Fig. 2). The rocks are medium to coarse-grained, gray to grayish dark in colour and mostly altered and deformed types to the extent that all gradation from the moderately massive to completely foliated types exist. Microscopic observation revealed coarse hypidiomorphic granular texture and disclosed main mineral phases in order of decreasing abundance; extremely altered (to sericite and chlorite) plagioclase, pleochoric prisms of hornblende, quartz (form about 10 %), oriented pale to dark-brown pleochoric biotite, sericite, chlorite, small columnar epidote, highly sericitized and discontinuously zoned k-feldspar, perthites, opaques, sphene, hexagonal apatite, actionlite, zircon and kaolin.

Granites and few micro-granites constitute only minor phases within the granodiorite sequence and believed to be emplacement products of the last intrusion phase to which the area was subjected. The granites are coarse to medium-grained, light to gray rocks; most of them are intensely deformed and sheared to the extent of foliation and partial destruction of the granitic features. Under the microscope, they show a porphyritic texture formed by pink K-feldspar phenocrysts in affine cloudy quartz and feldspar matrix associated with lesser amount of mafic minerals; sub-hedral flakey, brown biotite, green hornblende, chlorite, epidote and sericite and accessories of zircon, apatite and iron oxides.

2.5 Post-Orogenic Minor Intrusive rocks (Paleozoic / Early Mesozoic)

Commonly numerous quartz veins and lesser amounts of pegmatitic bodies together with scarce basic an acidic dykes are observed invading the country rocks throughout the area. Occurrence of these bodies with the associated alteration features suggests an intense hydrothermal activity. They are strongly deformed, broadly discordant, and irregular or lensiod bodies maintaining a common sinuous feature expressed mainly through swinging along N-S and NE-SW directions with steep dip westwards. In the field, the pegmatites seem to be older than most generations of quartz veins as they found terminating against some quartz veins.

The pegmatites are very coarse-grained massive rocks made up essentially of aggregates of coarse crystals of alkali-feldspar (orthoclase and microcline), quartz, some plagioclase, few mica flakes, tourmaline and apatite.

A number of scattered acidic and basic dykes are found cutting the different units of the basement complex. They are generally short and narrow bodies (0.5-1.0 m in width and rarely traceable for more than 3 m) occurring in contrast

colour with host rocks. Lithologically, typical granitic dykes (aplitic and granophyric) predominate, though dark and fine-grained basic dikes are also present.

The quartz veins represent an important episode in the history of the area since their emplacement was connected with the hydrothermal activities that brought about the gold mineralization. They are of variable sizes ranging from stringers, pods and narrow veins up to wide ones. A close examination reveals that more than a generation exists in the area; (1) the first one comprises early and widespread veins that are mainly concordant, deformed and folded with enclosing rocks (more than 200 m in length, few cm to 3 m width). The veins of this type exhibit varying colours, white, grey, milky, smoky, yellowish, brown, reddish or stained greenish depending on weather the quartz is pure, contaminated or stained by iron oxides or malachite. This type seems to be introduced along major structures and older shear zones. The veins are characterized by pinching and swell feature laterally and vertically and are associated with the main gold mineralization in Umtrambiesh area. (2) The second generation represents a younger phase of less abundant veins with more wider dimensions compared with the first generation, found striking in NW-SE or E-W direction, and occur as discontinuous, crashed and patchy bodies. This type of veins is often barren clean whitish quartz with some tourmaline crystals. Some smoky, gray and pink types are present.

2.6 The Sedimentary Cover (Mesozoic - Recent)

Sedimentary rocks assigned to the formally Nubian Sandstone Formation occur in the area as local outlier chiefly confined to a narrow land-strip stretched parallel to the eastern bank of the Nile. Most surface spreads of the formation are deeply covered with superficial deposits and loose rock screes. The sediments as else where, in he country, comprise undeformed, unmetamorphosed and bedded sequence that uncomfortably overlie the basement complex in a flat-lying attitude. Field and petrography revealed that the greater bulk of these sediments consist of medium to coarse-grained and variously cemented sandy facies of multi-colours (white, gray, dark, yellowish and brown), the coarser verities are always occupy the basal parts in fining upward sequence with rare true conglomerates.

Recent/Pleistocene superficial deposits uncomfortably overlie the above sediments and the underlying basement rocks. Gray to grayish dark heavy overburden of sandy clay and silty mud cover the Nile islands and the flood plains bordering it. The present-day beds of the dried-up streams have their floors covered by thin reddish to dark grayish loams and sandy clays of flush plain type mostly, coarse remnants of water-worn sediments comprising sub-angular to sub-rounded gravels.

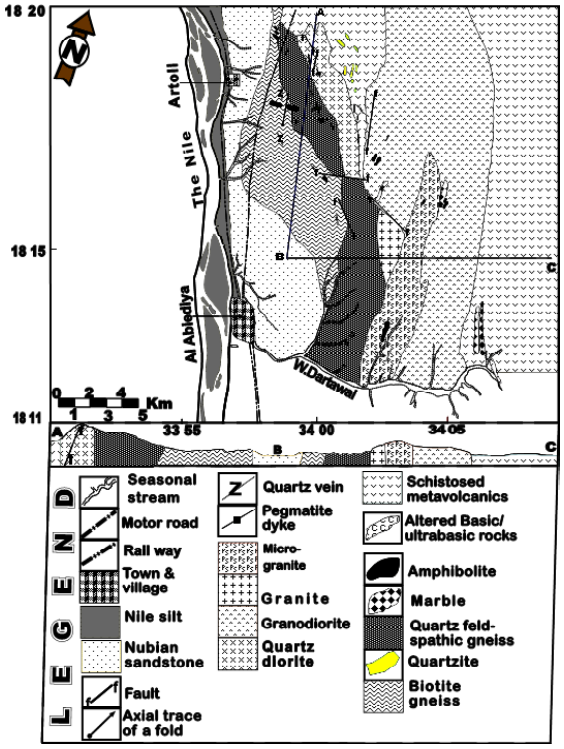

Figure 2. Geological map of the study area.

3. Material and Methods

Several representative samples encompassing the compositional and spatial range of metavolcanic rocks were collected during surface mapping from the Artoli area. Thirty-two samples were petrographically selected for whole-rock chemical analyses.

The samples were submitted through Rida Mining Company, Sudan to the ACME Analytical Laboratories, Vancouver, Canada for analytical work and calibration against international standards. The analytical results are listed in tables 1 and 2.

Whole rock element compositions were determined using inductively coupled plasma-atomic emission spectroscopy (ICP-ES) technique at ACME Analytical Laboratories, after lithium metaborate /tetraborate fusion and dilute nitric acid digestion of rock powder. Replicate analyses for some major and trace elements for some key samples were carried out by X-ray fluorescence spectrometry technique (XRF) following standard techniques and using a Phillips Venus 200 XRF instrument at the analytical laboratories of the Geological Research Authority of the Sudan (GRAS).

All major element values cited in table 1, and used in plots, were recalculated to 100 % on an anhydrous

basis. Loss on ignition (LOI) was determined from total weight loss after repeated ignition of the powdered samples at 100 °C for 1 hour and cooling. Satisfying analytical accuracy was achieved by using replicate analyses and compared with rock standards.

4. Rock Geochemistry and Tectonic Setting

The major, trace and rare earth elements abundance of the 32 whole-rock samples of the rocks believed to be metavolcanic from the area are shown in tables 1 and 2. These data are used in construction of several discrimination and variation diagrams in order to classify the rocks, decipher their geochemical nature and depict the tectonic setting of the area.

For specification of suitable discrimination and variation diagrams to be used, field and petrographic evidences were utilized in combination with geochemical data screening through TiO_2 versus SiO_2 diagram of Winchester and Max, 1984 and P_2O_5/TiO_2 vs. MgO/CaO diagram after Werner, 1987, both discriminated the rocks as of magmatic origin, (Fig. 3).

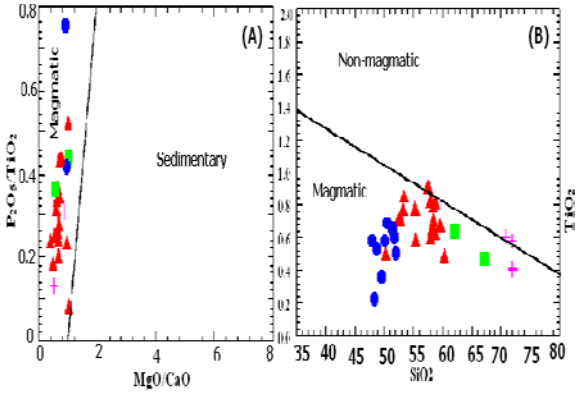

Figure 3. (A): P_2O_5 / TiO_2 vs. MgO / CaO diagram after Werner (1987); (B): SiO_2 vs. TiO_2 after Winchester and Max, 1984, diagram for discriminating between magmatic and non-magmatic rocks. *(Symbols: Closed triangle red ≈ Basalt, closed circle blue ≈ Andesite, closed cubic box green ≈ Dacite and cross pink ≈ Rhyodacite)*

4.1 Chemical Alteration and Element Mobility

In fact, all analyzed samples from the studied units are altered to some extent due to the low-grade metamorphism and/or extensive deformations, as reflected in the concentrations of the more mobile elements and the moderate loss on ignition (LOI) values (Table 1). Thus, it is likely that the present-day geochemical signature of these rocks may not be the same as the protoliths at the time of formation (Irvine and Green, 1976; Alfred and Michael, 1989**).** Therefore, and in order to elucidate the possible alteration effects of metamorphism and deformation, element mobility is noticed through plotting major and selected trace elements against Silica (SiO_2 wt %), Harker variation diagrams (Fig. 4), which show that compatible major oxides (MgO, TiO_2, Fe_2O_3t, MnO, Al_2O_3), P_2O_5 and CaO have normal, correlated and continuous differentiation trends, as they tend to decrease systematically with SiO_2 increases, (This suggests olivine, pyroxene, magnetite, and calcic plagioclase were major fractionating phases during evolution of the magma).

Sr, Ni, Zr, Y, Ba and Cr demonstrate no clear variation with SiO_2, where they remain nearly unchanged particularly in the acid varieties, thus they were probably immobile during metamorphism and other alteration processes. Some trace elements show slight gradual increase in their contents up to a maximum value of approximately 60 wt. % SiO_2 after which a decrease occurs with increasing SiO_2. It is evident from the figures 4-9 that, in spite of the low-grade metamorphism and deformation, some major and trace element signatures can be used for deciphering the original protoliths and tectonic environment.

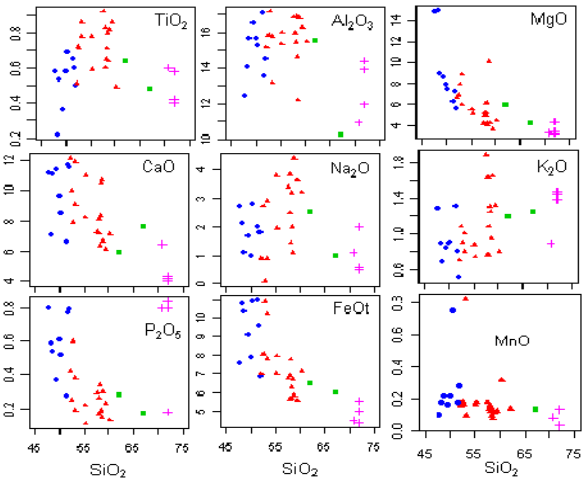

Figure 4. Harker variation diagrams; silica (SiO_2 wt %) plotted against a range of major (in wt %) for the metavolcanic rocks of the study area. *(Symbols: as in Figure 3)*

4.2 Major Element Characteristics

The major element chemistry data used with selected immobile trace and rare earth elements showed indicative characteristics, in spite of their known limited validity in classification schemes for altered and metamorphosed volcanic rocks (Alfred and Michael, 1989**)**.

Some major element concentrations span a wide compositional range (table 1), with silica SiO_2 (47.58 - 72 wt %), MgO (3.33 – 8.82 wt %) and MnO (0.03 - 0.82 wt %) suggesting diverse protolith.

Table 1. Major Elements Data of the Metavolcanic Rocks from Artoli Area

Sample	SiO_2	TiO_2	Al_2O_3	Fe_2O_3	MnO	MgO	CaO	Na_2O	K_2O	P_2O_5	L.O.I	Total
Amv1	70.78	0.60	10.93	4.96	0.08	3.33	6.44	1.11	0.89	0.80	1.5	101.42
Amv2	52.79	0.71	17.14	12.13	0.16	7.96	7.89	0.09	0.90	0.60	1.0	101.37
Amv3	72.00	0.40	14.39	4.85	0.03	3.23	4.19	0.59	1.39	0.84	1.6	103.51
Amv4	51.98	0.50	14.49	7.62	0.28	5.59	11.5	1.79	0.50	0.79	3.9	98.940
Amv5	51.70	0.60	13.50	10.6	0.17	7.29	11.71	1.77	0.80	0.77	1.5	100.41
Amv6	48.33	0.22	14.02	12.01	0.17	14.98	7.07	2.09	0.90	0.59	2.09	102.47
Amv7	49.58	0.36	16.46	10.10	0.16	8.53	11.37	1.65	0.84	0.37	1.9	101.32
Amv8	60.29	0.49	15.47	7.92	0.31	4.42	7.12	3.19	0.80	0.13	0.9	101.04
Amv9	53.28	0.86	13.15	11.36	0.09	8.82	11.88	0.90	0.80	0.38	0.8	102.32
Amv10	52.17	0.51	15.14	7.75	0.15	6.65	12.1	0.89	0.70	0.42	3.9	100.38
Amv11	50.10	0.58	15.64	8.77	0.22	7.91	9.66	0.98	0.90	0.61	3.5	98.870
Amv12	59.45	0.86	16.25	6.18	0.12	3.63	6.11	3.60	1.32	0.23	2.1	99.850
Amv13	52.50	0.72	15.83	8.98	0.18	6.88	9.98	2.72	1.08	0.25	0.6	99.720
Amv14	62.13	0.64	15.51	7.18	0.13	5.95	5.93	2.52	1.19	0.28	1.3	102.76
Amv15	55.18	0.78	15.35	7.80	0.16	5.53	8.21	3.79	0.88	0.22	1.3	99.200
Amv16	50.46	0.69	15.24	12.15	0.75	7.51	8.49	2.79	0.91	0.52	1.2	100.71
Amv17	58.58	0.64	12.18	7.43	0.07	10.12	10.7	1.10	0.95	0.15	0.8	102.72
Amv18	58.76	0.82	16.81	6.49	0.11	4.19	6.67	4.37	1.65	0.30	1.2	101.37
Amv19	47.90	0.58	12.42	8.43	0.10	14.82	11.15	2.69	1.29	0.80	0.5	100.68
Amv20	53.25	0.78	15.78	8.69	0.82	5.96	9.11	2.89	1.00	0.19	1.2	99.670
Amv21	72.00	0.42	11.96	6.14	0.03	4.33	4.31	0.50	1.45	0.80	0.5	102.44
Amv22	58.10	0.65	15.45	8.66	0.12	6.15	6.35	1.43	1.08	0.34	1.0	99.330
Amv23	58.34	0.71	16.84	6.98	0.13	4.19	8.32	3.17	1.31	0.18	0.3	100.47
Amv24	58.42	0.80	14.60	6.31	0.09	3.97	10.45	1.97	1.25	0.19	2.2	100.25
Amv25	67.13	0.48	10.27	6.64	0.13	4.23	7.60	1.00	1.25	0.17	2.6	101.50
Amv26	51.49	0.65	17.04	12.21	0.17	6.23	6.59	2.00	1.31	0.27	1.4	99.360
Amv27	72.00	0.58	13.89	5.55	0.13	3.39	4.01	1.99	1.48	0.18	0.9	104.10
Amv28	57.55	0.92	16.83	7.49	0.17	4.18	7.27	3.38	1.89	0.29	0.7	100.67
Amv29	55.33	0.59	16.00	8.86	0.17	5.12	10.97	1.93	0.74	0.11	1.0	100.82
Amv30	57.92	0.60	15.96	6.25	0.15	4.93	7.14	3.81	1.63	0.26	2.9	101.55
Amv31	48.69	0.53	15.64	11.51	0.22	8.93	11.07	1.10	0.69	0.54	1.3	100.22
Amv32	57.91	0.83	15.97	7.65	0.13	5.18	8.08	2.48	0.76	0.17	1.2	100.36

Table 2. Selected Trace and REE Abundances of the Metavolcanic Rocks from Artoli area

(The Sample of "-"symbol ≈ not analyzed)

Sample	Ni	Sc	Nb	Sr	Zr	Y	Ba	Hf	Cr	Th	La	Ce
Amv1	10	21	5	368	167	28	99	2.5	185	0.8	24.2	41
Amv3	10	15	9	223	115	16	129	1.5	435	2.1	25	35.9
Amv5	21	32	3	197	67	21	135	0.7	417	2.3	14.4	28.8
Amv7	53	45	6	134	63	14	114	1.9	418	1.23	17	36.98
Amv8	72	22	4	490	105	22	138	2.5	265	1.4	"-"	"-"
Amv9	10	22	8	443	124	29	102	2.2	287	2.2	32	49
Amv12	40.4	16	9	485	160	23	520	4.2	88	1.9	23.4	45
Amv13	65.1	18	4.8	522.7	66.5	20	282	3.7	183.4	1.3	"-"	"-"
Amv14	48	17	4	510	175	30	480	2.1	239	1.8	"-"	"-"
Amv15	93	6	6	365	85.7	22.1	231	2.17	226	3.1	10.1	20.5
Amv16	14	10	6	382	147	26	123	3.4	293	0.9	"-"	"-"
Amv17	21	22	4	398	175	24	350	2.7	279	2.3	"-"	"-"
Amv18	70.2	10	9.3	588.9	129	20	419	3.7	137	2.9	16	33
Amv19	12	12	5	222	129	32	370	1.9	298	1.3	"-"	"-"
Amv20	90.5	20	7	413	195	24	551	2.26	166	2.8	15.5	27.3
Amv21	35	12	6	225	97	29	256.4	0.98	189	0.7	"-"	"-"
Amv22	18	8	9	551	127	16	190	1.9	276	1.2	"-"	"-"
Amv23	22.3	26	6.3	268	95	24	193	2.3	53	2.4	12	25.3
Amv24	16	11	8	512	128	16	241	2.7	298	0.25	"-"	"-"
Amv25	17	13	6	395	115	21	248	1.6	389	1	"-"	"-"
Amv26	15	18	5	119	112	20	172	2.1	410	1.9	23.4	38.4
Amv27	17	7	9	501	185	41	187	1.7	418	0.9	"-"	"-"
Amv28	90	14	5.3	446	113	22.5	455.4	3.1	70.6	2.9	13.9	27.4
Amv29	30.1	13	2.9	179.8	87	15	118	0.9	78	0.82	20.3	35.6
Amv30	82.5	43	9	790	106.8	26.6	589.2	3.2	149	2.9	32	42.6
Amv31	12	10	7	248	52	18	122	1.8	319	1.6	"-"	"-"
Amv32	78.7	26	4.15	193.4	62	18.5	100.4	1.9	277	1.2	25.8	42.7

Table 2—Continued

Sample	Pr	Nd	Sm	Eu	Gd	Tb	Dy	Ho	Er	Tm	Yb	Lu
Amv1	6.1		4.3	0.95	3.45	0.5	2.9	0.61	1.8	0.3	2.15	0.4
Amv3	5.6	23.9	4.5	1.2	2.67	0.36	2.79	0.57	1.6	0.41	2.4	0.39
Amv5	3.55	14.3	3.61	1.1	2.7	0.4	2.6	0.5	1.8	0.3	2.3	0.37
Amv7	4.61	18.4	3.9	1.2	3	0.62	3.21	0.69	2.1	0.3	2.1	0.3
Amv9	7.68	28	7.1	1.6	5.1	0.71	2.3	0.4	1.3	0.29	1.2	0.22
Amv12	6.7	26.2	5.5	1.3	3.9	0.7	4	0.65	2.4	0.31	2.2	0.3
Amv15	2	12	3	1	3.1	0.4	3.8	0.6	2	0.24	2.4	0.45
Amv18	4.2	17.8	4	0.86	3.6	0.69	3.9	0.7	1.9	0.3	1.3	0.4
Amv20	2.8	15.9	3.7	1.2	3.6	0.7	3.2	0.8	2.4	0.4	2.1	0.32
Amv23	2.7	12.8	3.1	0.9	3.4	0.6	3.5	0.9	2.2	0.31	2.3	0.35
Amv26	4.8	14	5.1	1.1	4.5	0.6	4	0.7	1.7	0.4	2.3	0.41
Amv28	3.1	15.7	3.7	1.4	3.8	0.51	3.7	0.8	2.3	0.34	2.4	0.4
Amv29	4.7	14.6	2.3	0.8	1.8	0.32	2.1	0.5	1.4	0.2	1.6	0.25
Amv30	6.5	28	7.1	1.5	4.1	0.7	3.4	0.81	1.9	0.36	1.7	0.35
Amv32	5.3	16.6	2.3	0.73	2.4	0.32	2.3	0.45	1.78	0.3	2.2	0.34

Most samples show high-alumina (Al_2O_3) contents from 10.27 wt % up to 17 wt %, (mean 15.41wt %) values similar to those of calc-alkaline series rocks. Iron content (Fe_2O_3) seems to be relatively high ranging between 4.85 and 12.21 wt %, but only few samples have Fe_2O_3 contents > 12 wt % and Fe_2O_3/MgO range < 2. The high iron contents appear to reflect an abundant secondary opaque phase (magnetite?). TiO_2 values are generally < 1 %, therefore they are in the range accepted in calc-alkaline lavas (Irvine and Baragar, 1971; Pearce and Cann, 1973).

The majority of samples show relative high abundance of CaO ranging between 4.19 to less than 12 wt % which may be related to the presence of epidote and the non-intensive metamorphism (Jakes and White, 1972).

The abundances of Na_2O (mostly 0.59 – 4.37 wt %), K_2O (0.5 – 1.89 wt %), P_2O_5 (0.11–0.84 wt. %) and the Na_2O/K_2O (mostly between 1 and 3) are low compared to typical values of Jakes and White, 1971 for calc-alkaline rocks, this can surely be attributed to a loss during alteration and metamorphism. The ratios of Zr/TiO_2, Fe_2O_3/MgO and TiO_2/K_2O displayed by the rock samples are consistent with the range given by most sub-alkaline volcanic rocks of basic to intermediate composition (Pearce and Cann, 1973; Winchester and Floyd, 1977).

4.3 Trace and Rare Earth Elements Characteristics

In terms of trace elements content (Table 2), With the exception of Sr (119-790 ppm), Y (14-40 ppm) and La (12- 26.4 ppm), their abundance is generally low Nb (2 -9 ppm), Ba (99- 589 ppm), Th (0.8-2.9 ppm), Ni (10 – 90 ppm) and Zr (62-207 ppm), feature suggesting the generation of these rocks within active plate margin (Pearce and Gale, 1977). The Cr abundances is generally low (53 -300 ppm), but some samples contain comparatively high Cr content (315- 435 ppm)

The ratios of (Niobium with Yttrium) Y/Nb and Nb/Y fall in the range between 0.83 -5.75 and (0.1-0.6) respectively, Nb/Y and La/Sc ratios are mostly < 1.0 and La/Th (5- 30.3), La/Y (0.5- 1.6) implying possible approach to clac-alkaline and tholeiitic affinities (Y/Nb always < 1.0 in typical to clac-alkaline and tholeiitic basalts, Garcia, 1978).

4.4 Magma Characterization

Noting the trend displayed by the sample sets and sample falling in a specific field in the total alkali versus silica diagram of Le Bas, et al., 1986 (Fig. 5A) it is clear that the samples of the metavolcanic rocks are principally identified as low-silica andisites (53– 57 wt. % SiO_2), and only a few samples fall in the basalt field and the felsic samples are dacites. In the plot using immobile elements Nb/Y versus Zr/TiO_2 of Winchester and Floyd 1977 (Fig. 5B), the mafic samples fall in the andesite and the basalt/andesite fields, consistent with their classification in Figure 5A. However, most of the felsic samples plot in the andesite field rather than the dacite field.

For the magma type, the silica versus total alkali discrimination diagram of Irvine and Baragar, 1971(Fig 6A), defines distinct trend of sub-alkaline affinity for all samples, and the same fact is also confirmed by the (Na_2O+K_2O) vs. SiO_2 diagram after Le Bas, et al., 1986, (Fig. 5A). The K_2O vs. SiO_2 plot after Peccerillo and Taylor, 1976 (Fig, 6B), which straddle the tholeiitic and calc-alkaline boundaries indicates that the petrochemical composition of metavolcanic rocks fall within the calc-alkaline field.

In the multi-element diagram (Fig. 7) normalized to primitive mantle values of McDonough and Sun (1995), the trace element data show that the rocks possess a typical calc-alkaline island arc trace element patterns, enriched incompatible large ion lithophile elements (LILE: Sr, Ba, and K) relative to high field strength elements (HFSE: Zr, Hf, Y, Ti, and Nb) contents, that show a negative Nb and Ni anomalies.

In the chondrite-normalized REE pattern (Fig. 8), values of Sun and McDonough, 1989), all the analyzed rocks samples display enrichment in fractionated light rare earth element (LREE: La, Ce, Pr, Nd and Sm) contents relative to heavy rare earth elements (HREE: Tb, Dy, Ho, Er, Tm, Yb and Lu) contents. The Pattern is generally steep, moderately strong enrichment right-inclined type and lack Eu-anomalies similar to those from calc-alkaline series.

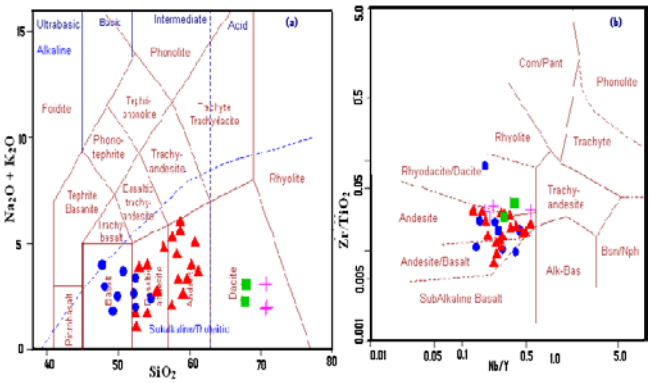

Figure 5. Chemical classification diagrams of the Artoli metavolcanics based on TAS (wt %) (Na_2O + K_2O vs. SiO_2) of Le Bas, et al., 1986 and Nb/Y-Zr/TiO_2 of Winchester and Floyd 1977. *(Symbols: as in Figure 3)*

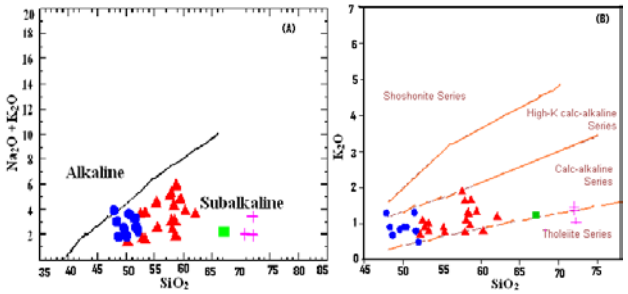

Figure 6. (A) The silica versus total alkali plot (Series boundaries after Irvine and Baragar, 1971) and (B) Weight percent K_2O vs. SiO_2 plot (Series boundaries are after Peccerillo and Taylor, 1976) illustrating clac-alkaline trends in the Artoli metavolcanic rocks. *(Symbols: as in Figure 3)*

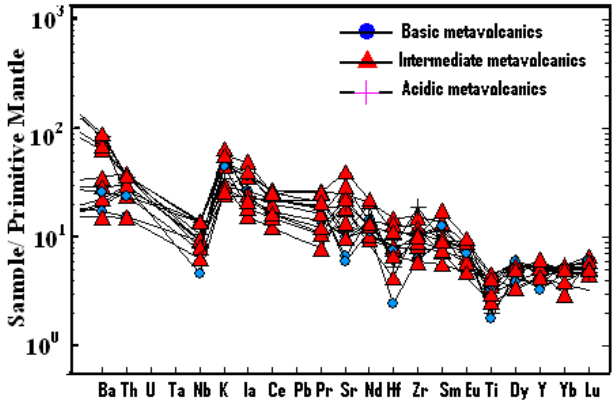

Figure 7. Mantle-normalized multi-element diagram of the bulk rock samples from the study area, (McDonough and Sun, 1995).

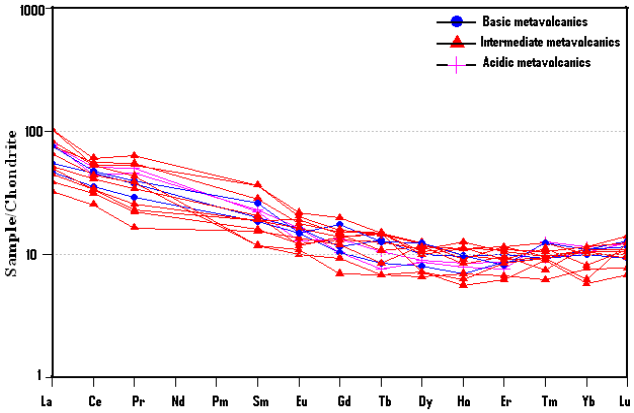

Figure 8. Chondrite-normalized REE patterns for the Artoli metavolcanics, chondrite normalization values are from Sun and McDonough (1989).

4.5 Geotectonic Setting

Samples were plotted on three immobile elements' geochemical diagrams that are proved to be effective in discriminating tectonic settings of volcanic rocks.

Plotting the immobile elements that preserve their abundance through post-formational processes following Müller, et al., 2001, in Zr vs. Y diagram, all samples discriminated as subduction-arc related rocks (Fig. 9A). In the Th-Hf-Nb tertiary discrimination diagram of Wood, 1980, most of the metavolcanic rocks (except three) plot in the calc-alkaline lavas subfield (Fig. 9B), but in the Zr vs. Ti tectonomagmatic discrimination diagram of Pearce and Cann, 1973, samples plot exclusively in the island arc calc-alkaline lavas field (Fig. 9C).

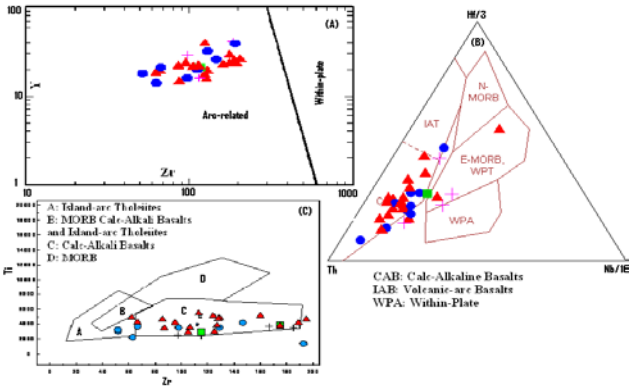

Figure 9. (A) Zr vs. Y Biaxial geochemical discrimination diagram indicating the subduction-arc features (Müller, et al., 2001), (B): Th-Hf-Nb triangular discrimination diagram (Wood 1980) and (C): Zri vs. Ti (Pearce and Cann , 1973) showing the inferred tectonic setting of the study area. *(Symbols: as in Figure 3)*

5. Discussion and Conclusions

The geological setting of the Artoli area, which characterized by predominantly low-grade metavolcanic rocks and minor high-grade metasediments is obviously different form that of the adjacent Bayuda terrane to the west (Saharan Metacraton) and the Keraf petrotectonic assemblage to the north (Suture zone), as the former is heterogeneous continental crust of high-grade gneisses, migmatites and supracrustal rocks of ensialic geochemical affinities and the latter is dominated by siliciclastic and carbonate-rich low-grade metasediments, ophiolitic nappes, and molasse-type sediments.

The dominant metamorphic rocks are from volcanic protoliths as disclosed from the field, petrographic work and geochemical petrogenesis signature (Fig. 3). It is likely that the alteration have not caused substantia1 mobility of element present in the original protoliths as reflected by the normal, correlated and continuous differentiation trends (though some show broad scatter variation) in Harker silica variation diagrams (Fig. 4) which may indicates original source. Thus, major element can be used

together with the alteration resistant trace and rare elements in classifying rocks and identifying the paleotectonic setting.

The characteristics of the major elements (a relative decrease in Al_2O_3, Fe_2O_3 MgO with silica increase, and high Al_2O_3 low TiO_2) and chemical classification diagrams (Fig. 5) confirm what was suspected from field and petrographic work, the existence of a volcanic suite consisting of basic, intermediate and intermediate-acid rock types, with fractionated rocks predominance, especially andisites, basaltic-andisites and dacites with lesser amount of basalts.

A distinctly sub-alkaline affinity is a characteristic feature of these rocks as indicted by the magma type discrimination diagrams (Fig. 6). Most element concentration features displayed by the metavolcanic rocks samples are those assigned to the characteristic features of island arc calc-alkaline rocks, among these are; the marked variation in silica content, the low values of TiO_2 (generally < 1), low Cr, Nb, Ba, Th, Ni and Nb/Y ratios (< 1.0), and the high alumina Al2O3 content (Tables 1&2), moreover, Fe2O3t, MgO, TiO2, CaO decrease systematically with increasing SiO2 (Fig. 3). The clear calc-alkaline geochemical signature is also inferred from the predominance of high proportion of basaltic andesite and andesite fractionated rocks (Fig. 5). The enrichment of large-ion lithophile elements (LILE) and light rare earth element (LREE) contents relative to heavy rare earth elements (HREE) and high field strength elements (HFSE) contents (Rollinson, 1993 and Bloomer et al., 1995), steep moderately strong right-inclined enrichment type pattern and the negative Nb-Ti anomalies (Figs. 7 & 8) all are confirming evidences.

The prominent negative Nb-Ti in spider diagrams for all samples, low Cr and Ba coupled with depletion in Y and Zr postulate subduction environment (Jakes and White, 1972; Shandelmeir et al., 1994b). The predominance of calc-alkaline andesitic rock suites suggests that, the rock series in the area are compatible with products of plate margin tectonic settings of the island arc environment, a fact confirmed by the discrimination and spider diagrams used (Figs. 5-8).

Based on the above account, a conclusion can be reached with the following outlined points derived from the field and petrographic observations combined with the interpretation of element concentrations and trends revealed by the discrimination and variation diagrams:

(1) The area under consideration is a regionally metamorphosed terrane, the rocks of which have been subjected to low-grade metamorphism and/or alterations, the dominant metamorphic rocks are from volcanic protoliths. Although, metamorphism have destroyed most original igneous features, a relationship between the geochemical groups and field characteristics is obvious, this will be helpful in separating and mapping the rock units.

(2) Fractionated rocks are the dominant among the Artoli metavolcanics, as more than two-thirds of the rocks are andesites and basaltic andesites and the remainder are dacites and basalts.

(3) Petrographic and geochemical results give clear evidences that distinctly sub-alkaline affinity is a characteristic feature of these rocks, which are dominated by calc-alkaline suites.

(4) The predominant clear calc-alkaline andesitic rocks, the LREE fractionation compared to the HREE and the enrichment of LILE relative to HFSE contents along with element contents suggest the generation of the protoliths of the metavolcanic rocks of the area in a tectonic environment of island arc setting a fact which testified by the various geochemical diagrams used.

(5) The overall geological and geochemical characteristics of the Artoli metavolcanic rocks disclosed by our study have provided essential evidence to consider the area as part of the westernmost Nubian Shield, because the features are consistent with the arc accretion models postulated in Sudan, Egypt and Saudi Arabia for the Neoproterozoic evolution of the Arabian-Nubian Shield.

Acknowledgements

The financial support for this work was provided by Dongola University. We would like to acknowledge the Department of Geology and Mining, University of Juba, for logistical support during the fieldwork, the Geological Research Authority of Sudan (GRAS) for the facilities offered in carrying out petrographic investigation and XRF analyses and the Rida Mining Company, Sudan who covered most of the cost of whole-rock geochemical analyses from Acme Labs. The authors wish to acknowledge with great thanks Prof. Dr. He Sheng of China University of Geosciences (Wuhan) for his valuable discussion, comments and constructive remarks on the manuscript. The authors sincerely thank Adli A/ Majeed, Madani Rajab, Dr. A/ haman Ahmed and Dr. Mutasim Adam for their contribution during field mapping.

References

1. **Abdel Rahman,** E. M., **1993**. Geochemical and geotectonic controls of the metallogenic evolution of selected ophiolite complexes from the Sudan. Berliner

geowissenschaftliche Abhandlungen. 145 (A): 145-175.
2. **Abdelsalam,** M. G., Liegeois, J. P. and Stern, R. J., **2002**. The Saharan Metacraton. J. Afr. Earth Sci. 34:119–136.
3. **Alfred,** J. E. and Michael, G. D., **1989.** Discrimination between altered and unaltered rocks at the Connemarra and Kathleen Au deposits, western Australia. Jou. Geochem. Explor. 31: 237-252.
4. **Almond**, D. C., **1982**. New ideas on the geological history of the Basement Complex of NE Sudan. Sudan Note and Rec. 59: 106-136.
5. **Bloomer**, S. H., Taylor, B., MacLeod, C. J., Stern, R. J., Fryer, P., Hawkins, J. W. and Johnson, L. E., **1995**. Early arc volcanism and the ophiolite problem: A perspective from drilling in the western Pacific. Geophysical Monograph, American Geophysical Union. 88: 1-30.
6. **Fitches,** W. R., Graham, R. H., Hussein, I. M., Rise, A. C., Shackleton, R. M. and Price, R. C., **1983.** The Late Proterozioc ophiolites of Sole Hamed, NE Sudan. Precambrian Res. 19: 358-411.
7. **Garcia,** M. O., **1978.** Criteria for identification of ancient volcanic arc. Earth and Planetary Science Letters. 14: 147–165.
8. **Harker,** A. **1909.** The natural history of igneous rocks. Macmillan, New York.
9. **Hussein,** I. M., Kröner, A., and Durr, S. T., **1984**. Wadi Onib: A dismembered Pan-African Ophiolite in the Red Sea Hills of Sudan. Bull. Faculty of Earth Science, King Abdulaziz Unv., Jeddah. 8: 523-548.
10. **Irvine**, I. J. and Green. H., **1976**. Geochemistry and Petrogenesis of the newer baslts of Victoria and South Australia. Journal of Geol. Soc. of Australia. 23 (2): 45.
11. **Irvine**, T. N. and Barager, W. R. A., **1971**. A guide to the chemical classification of the common volcanic rocks. Canadian Journal of Earth Science. 8: 523-548.
12. **Jakes**, F. and White, A. J. R., **1971**. Composition of island arcs and continental growth. Earth Planet. Sci. Lett. 12: 224-230.
13. **Jakes**, P. and White A. J. R., **1972**. Major trace element abundances in volcanic rocks of orogenic areas. Geol. Soc. Am. Bull. 83: 29–40.
14. **Kennedy**, W. Q., **1964**. The structural differentiation of Africa in the Pan-African (+ 500 my) episode. University of Leeds Research Institute of African Geology, Department of Earth Sciences Annual Report. 8: 48-49.
15. **Kröner,** A., **1984.** Late Precambrian plate tectonics and orogeny: a need to redefine the term Pan-African. In: Klerkx, J. and Mishot, J., Editors, 1984. Afr. Geol., Tervuren, Belgium. pp. 23–28
16. **Kröner**, A., Greiling, R., Reischmann, T., Hussein, I. M., Stern, R. J., Durr, S. and Zimmer, M., **1987a**. Pan-African crustal evolution in the segment in the northern Africa. In: Kro¨ner, A. (Ed.), Proterozoic Lithosphere Evolution. International Lithosphere Program Publication 130. American Geophysical Union Geodynamics Series, Washington, DC. 17: 235–257.
17. **Küster**, D. and Liegeois, J. P., **2001**. Sr, Nd isotopes and geochemistry of the Bayuda Desert high-grade metamorphic basement (Sudan): an early Pan-African oceanic convergent margin, not the edge of the East Saharan ghost craton? Prec. Res. 109: 1–23.
18. **Le Bas,** M. J., Le Maitre, R. W., Streckeisen, A. and Zanettin, B. **1986.** A chemical classification of volcanic rocks based on the total alkali–silica diagram. Journal of Petrology. 27: 745–750.
19. **McDonough**, W. F. and Sun, S. S., **1995**. The composition of the earth. Chemical Geology. 120: 223-253.
20. **Müller**, D., Franz, L., Herzig, P. M. and Hunt, S., **2001**. Potassic igneous rocks from the vicinity of epithermal gold mineralization, Lihir Island, Papua New Guinea. Lithos. 75: 163-186.
21. **Pearce**, J. A. and Cann, J. R., **1973**. Tectonic setting of basic volcanic rocks determined using trace element analyses. Earth and Planetary Science Letters. 19: 290–300.
22. **Pearce,** J. A. and Gale, G. H.**, 1977.** Identification of ore deposition environments from trace element geochemistry of associated igneous host rocks. Geol. Soc. Spec. publ. 7: 14-24.
23. **Peccerillo,** A. and Taylor S. R., **1976**. Geochemistry of Eocene calcalkaline rocks from Kastamonu area northern Turkey. Contributions to Mineralogy and Petrology. 68: 63-81.
24. **Rollinson**, H. R., **1993.** Using geochemical data: Evaluation, presentation, interpretation: Longman Group UK Ltd. 352 p.
25. **Schandelmeier**, H., Abdel Rahman, E. M., Wipfler, E. K., uster, D., Utke, A. and

Matheis, G., **1994b**. Late Proterozoic magmatism in the Nakasib suture, Red Sea Hills, Sudan. J. Geol. Soc. Lond. 151: 485–49.

26. **Stern**, R. J., **1994**. Arc assembly and continental collision in the Neoproterozoic East African Orogen: Implications for the consolidation of Gondwanaland. Ann. Rev. Earth Planet. Sci. 22: 319-351.
27. **Stern**, R. J., **2002**. Crustal evolution in the East African Orogeny: geodynamic isotopic prospective. J. Afr. Earth Sci. 34: 109–117.
28. **Stern**, R. J., Kröner, A., Bender, R. T., Reischmann, and Dawoud, A. S., **1994.** Precambrian basement around Wadi Halfa, Sudan: a new perspective on the evolution of the Eastern Saharan Craton. Geologische Rundschau. 83: 564-577.
29. **Sun,** S. S., and McDonough, W.F., **1989.** Chemical and isotopic systematics of oceanic basalts: Implications for mantle composition and processes, in Saunders, A.D., and Norry, M.J., eds., Magmatism in the ocean basins: Geological Society [London] Special Publication. 42: 313–345.
30. **Winchester,** J. A. and Floyd, P. A., **1977**. Geochemical discrimination of different magma series and their differentiation products using immobile elements. Chemical Geology. 20: 325–343.
31. **Winchester**, J. A. and Max, M. D., **1984.** Geochemistry and origin of the Annagh Division of the Precambrian Erris complex, NW County, Mayo, Ireland. Precambrian Ress. Amsterdam. 25: 397–414.
32. **Wood**, D. A., **1980**. The application of a Th–Hf–Ta diagram to problems of tectonomagmatic classification and to establishing the nature of crustal contamination of basaltic lavas of the British Tertiary volcanic province. Earth and Planetary Science Letters. 50: 11–30.

April 26, 2010